

Micromechanical Parameters, Alloying ability, Growth Habits and Thermo Stability of Aluminium Rich Al-Cd-Pb-Bi Composite

Parshotam Lal.

Member, Department of Chemistry, ISCAS Institute of Solid State and Materials Science
Jammu University Campus, Jammu, India

ABSTRACT: The current work is conducted with an aim to accrue comprehensive understanding of the growth habits of an analog of aluminium rich composites from the melt to explore the superiority of micromechanical parameters in the domain of anisotropic alignment of microstructural parameters. Homogeneous chemical composition and liquidus temperature of the fabricated composite Al-Cd-Pb-Bi are ascertained by DSC and alloying ability of the constituent phases is established by X-ray diffraction study. X-ray diffraction studies affirm composite alloys to be a terminal solidus solution of physically distinct and mechanically separable phases. The scanning electron microscope is used in the analysis of surface structures of the composite phases at variable anisotropic growth rates. Computed Vickers micromechanical parameters of the composite at variable growth velocity under constant applied load 50×10^{-2} N in the experimental load range 10×10^{-2} N to 100×10^{-2} N for a definite time interval 10s, are found to follow an identical form of the Weibull probability distribution curve. Naturally occurring constants with the micromechanical parameters are extensively studied for physical understanding of the plastic deformation.

KEYWORDS: property combination, moderate growth, aligned lamellae, fracture toughness, plastic deformation.

I. INTRODUCTION

Many alloying composite materials, being in service, are subjected to forces or loads; example includes the aluminium alloy from which an airplane wing is constructed and steel in an automobile axle. In such situations, it is necessary to know the characteristics of the material and to design the member from which it is made such that any resulting deformation will not be excessive and fracture will not occur. The mechanical behaviour of a material reflects the relationship between its response and deformation to an applied load or force. Important mechanical properties are strength, hardness, ductility and stiffness [1-5]. The mechanical properties of materials are ascertained by performing carefully designed laboratory experiments that replicate as nearly as possible the service conditions. Factors to be considered include the nature of the applied load and its duration, as well as the environmental conditions. It is possible for the load to be tensile, compressive, or shear, and its magnitude may be constant with time, or it may fluctuate continuously. Application time may be only a fraction of a second, or it may extend over a period of many years. Service temperature may be an important factor. Hardness [6-7] is an important mechanical property that measure of a material's resistance to localized plastic deformation (e.g., small dent or a scratch). Hardness test are performed more frequently than any other mechanical test for three reasons: Firstly, they are simple and inexpensive – ordinarily no special specimen need be prepared, and the testing apparatus is relatively inexpensive. Secondly, the test is nondestructive the specimen is neither fractured nor excessively deformed; a small indentation is the only deformation and third mechanical properties often may be estimated from hardness data, such as tensile strength. Quantitative hardness techniques have been developed over the year in which a small indenter is forced into the surface of a material to be tested, under controlled conditions of load and rate of application. The depth or size of the resulting indentation is measured, which in turn is related to a hardness number; the softer the material, the larger and deeper is the indentation,

International Journal of Innovative Research in Science, Engineering and Technology

(An ISO 3297: 2007 Certified Organization)

Website: www.ijirset.com

Vol. 6, Issue 2, February 2017

and the lower the hardness index number. Measured hardness are only relative (rather than absolute), and care should be exercised when comparing values determined by different techniques.

II. MATERIALS AND METHOD

The composite alloy Al-Cd-Pb-Bi was prepared in the pyrex tube by weighing a proper amount of purity 99.999% Al [Alfa Aesar, AR, mp 949 K, $\Delta_f H = 10.80 \text{ kJmol}^{-1}$], 99.999% Cd [Alfa Aesar, AR, mp 597 K, $\Delta_f H = 6.19 \text{ kJmol}^{-1}$], 99.999% Pb [Alfa Aesar, AR, mp 584 K, $\Delta_f H = 4.70 \text{ kJmol}^{-1}$] and 99.999% Bi [Alfa Aesar, AR, mp 551 K, $\Delta_f H = 11.20 \text{ kJmol}^{-1}$] shots with 40 wt% Al, 20 wt% Cd, 20 wt% Pb and 20 wt% Bi. The melting temperatures and enthalpies of fusion of the constituent metals, cited in the parentheses, were obtained by thermal analysis approaching very closely to their literature values. The ampoule tube was sealed under vacuum to avoid oxidation and infused in a furnace set a temperature $\sim 900 \text{ K}$ for alloying Al, Cd, Pb and Bi metals to Al-Cd-Pb-Bi composite. Homogeneity of the composite was ensured by heat-chill process keeping the temperature of the heater (air oven) $\sim 700 \text{ K}$ and that of the cooler (water bath) $\sim 300 \text{ K}$. The liquidus temperature of the composite alloy Al-Cd-Pb-Bi (370 K) was also ascertained by thermal analysis.

i) Anisotropic growth

The experimental composite alloy Al-Cd-Pb-Bi was subjected to oriented growth in the following experimental setup. An experimental sealed pyrex tube containing half-full melt of a freshly prepared composite was clamped to the centre of an empty graduated beaker (volume capacity $\sim 1 \text{ dm}^3$) manipulated midmost in an air oven set at a temperature 30K higher than its liquidus temperature. The molten mass in the tube was nucleated by circulating silicone oil at 18 different intervals spanned in the time range 50-60 min. from the oil reservoir perforated and plugged with a glass tube carrying valve to control the percolation at $\sim 300 \text{ K}$. The melt in the tube started nucleating when the rising level of the oil just touched the bottom of the tube. Many a sample of the composite was grown anisotropically at different but nearly consistent growth rates determined by circulating approximately the same volume of the oil for each selected interval. The anisotropic solidification process offers mechanically efficient lamellae structure of the composite called 'modal product' at the moderate growth mode ($\sim 2.90 \times 10^{-7} \text{ m}^3 \text{ s}^{-1}$).

ii) Instantaneous solidification

Isotropic growth was performed by immersing an experimental pyrex tube containing the composite melt in an ice bath maintained at $\sim 273 \text{ K}$. The growth being instantaneous in nature is presumed of zero order. Likewise, several samples of composite phases were solidified for the isotropic growth for observations.

iii) Microscopic studies

The specimen grown anisotropically and isotropically were polished at room temperature following a procedure similar to that adopted for analogous problem. To reveal the microstructure, a thin layer of the specimen etched in ferric chloride was mounted on stub with gold-coated holder and examined under a scanning electron microscope for microgrowth observation. Many samples of each specimen were viewed in this manner and the growth habits of the growing phases during solidification [8-10] at different growth rates were accordingly photographed.

iv) Vickers test

Indentations were induced on selected points chosen diagonally on an anisotropically or instantaneously grown composite sample at room temperature ($\sim 300 \text{ K}$), using a Vickers microhardness tester attached to an incident-light metallurgical research microscope in the applied load ranging from 10×10^{-2} to $100 \times 10^{-2} \text{ N}$. For each test, a very small diamond indenter having pyramidal geometry was forced into the surface of the specimen at room temperature and the size of the indent was found growing with rising applied load. Vickers micromechanical parameter of composite alloy Al-Cd-Pb-Bi was computed by the following relation [11-14]:

Vickers hardness, $H_v = \frac{1.8544P}{d^2}$ ----- (1) where P is the applied load in Newton force and d is average diagonal length of the indentation mark in meter. The parameter P depends on both the size of specimen being

tested and the nature of the test, while d varies with the size of the crack. Experimental evidences are such that they emblematically acknowledge the unique mechanical property of the modal product.

v) X-ray diffraction studies

The X-ray diffraction patterns exhibited by the experimental composite phases were recorded with Diffraction [12] System-XPRT=PRO using $\text{CuK}\alpha$ radiation of wavelength 1.5408 \AA at room temperature. The powder X-ray was recorded in a 2θ range of 5° to 90° with the step size of 0.05 and step time of 1s .

III. RESULTS AND DISCUSSION

The DSC curve resulted in by the thermal analysis of the composite alloy Al-Cd-Pb-Bi is presented in Fig. 1 explicitly exhibiting its thermal stability, homogeneity and liquidus temperature.

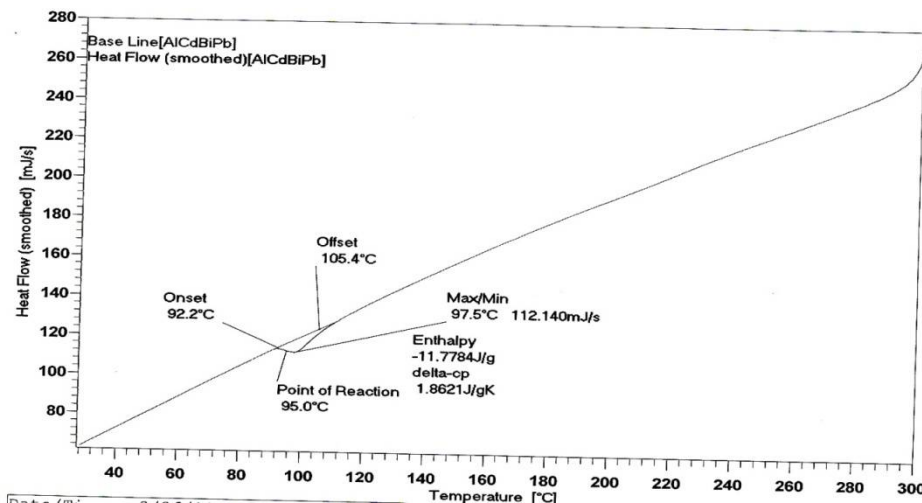


Fig. 1: DSC curve of composite alloy Al-Cd-Pb-Bi.

Micromorphological images of the composite phases oriented at different growth rates are pictorially displayed in Fig.2. The mutual tendency of the lamellae alignment microstructural parameters of the composite in the anisotropic growth process presents their relationship with mechanical aptitude. Micromechanical parameter is found most probable at the moderate anisotropic growth ($\sim 2.90 \times 10^{-7} \text{ m}^3 \text{ s}^{-1}$) which a unique finding in the present work searched out in the experimental growth observations by setting the flow- interval of silicone oil at $5.0 \times 10^{-4} \text{ m}^3$ for 28 min, this particular process of solidification strengthens the composite lamellae to exhibit optimum mechanical ability in the present investigation.

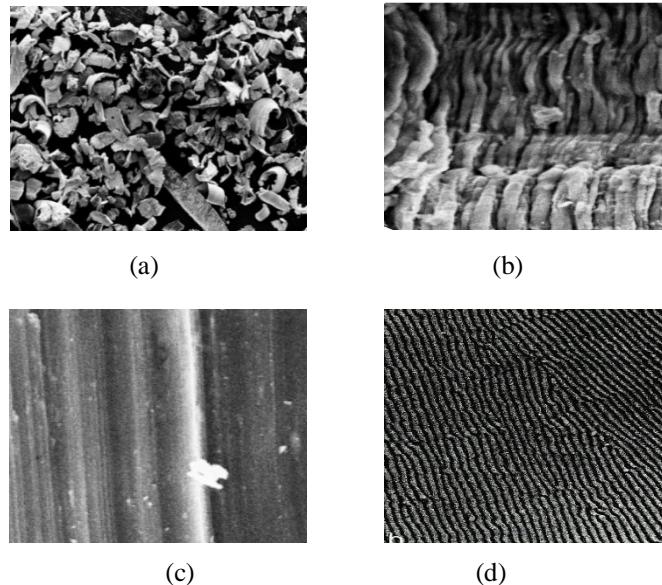


Fig. 2. Micromorphological of the composite Al-Cd-Pb-Bi (1500x).

- (a) Distorted microstructure (isotropic) of composite phaselamellae in ice bath at ~273 K(fast growth region)
(b) Evolution of composite phase lamellae in growth direction from bottom to top in the slow growth region, $1.50 \times 10^{-7} \text{ m}^3 \text{ s}^{-1}$;
(c) and (d) Lamellar composite phase, growth direction from bottom to top at moderate anisotropic growth $2.90 \times 10^{-7} \text{ m}^3 \text{ s}^{-1}$

Figure 2 indicates the ability of the moderate anisotropic growth ($\sim 2.90 \times 10^{-7} \text{ m}^3 \text{ s}^{-1}$) in producing and putting strong, stiff, lamellae of the composite in the right place, in the right orientation with right volume fraction resulting in thereupon the formation of its modal product Fig.2d. Evidentially, the modal product at the aforementioned anisotropic growth attain lamellar structure comprising of strong lamella-matrix bond in comparison to slow and fast growth process producing fragile matrix because of the aggressive, non attaching and crossing develop habits of the lamellae responsible for its distorted structures Fig 2 (a-c). The indentation impressions inflicted composite specimens solidified at variable anisotropic growth rates (18 intervals) selected in the present work with a constant load of $50 \times 10^{-2} \text{ N}$ for indentation time 10s were subsequently subjected to micromechanical tests under Vickers microhardness tester [15-20] and the variation of computed micromechanical parameters thereof in the experimental growth range strictly follow the Weibull probability distribution curve Fig.3. Verily, the curve is an important deduction of the linear; nonlinear and linear variant mechanical-growth inflexions in the slow; moderate and fast growth regions respectively. The microstructural parameters seem to follow the Weibull distribution in both the slow and fast growth resulting in their random habits. On the contrary the microstructural parameters for tendering to follow the Gauss distribution by arranging themselves in preferred alignment. The moderate region of the curve paves the formation of modal microstructure of the composite appropriately called the modal product.

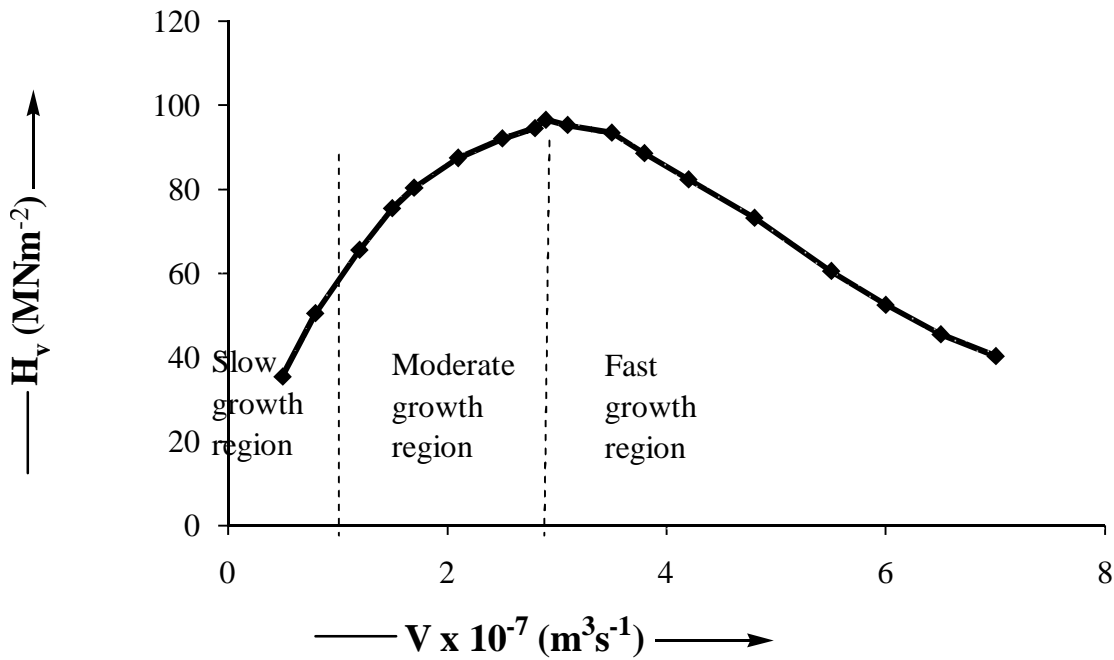
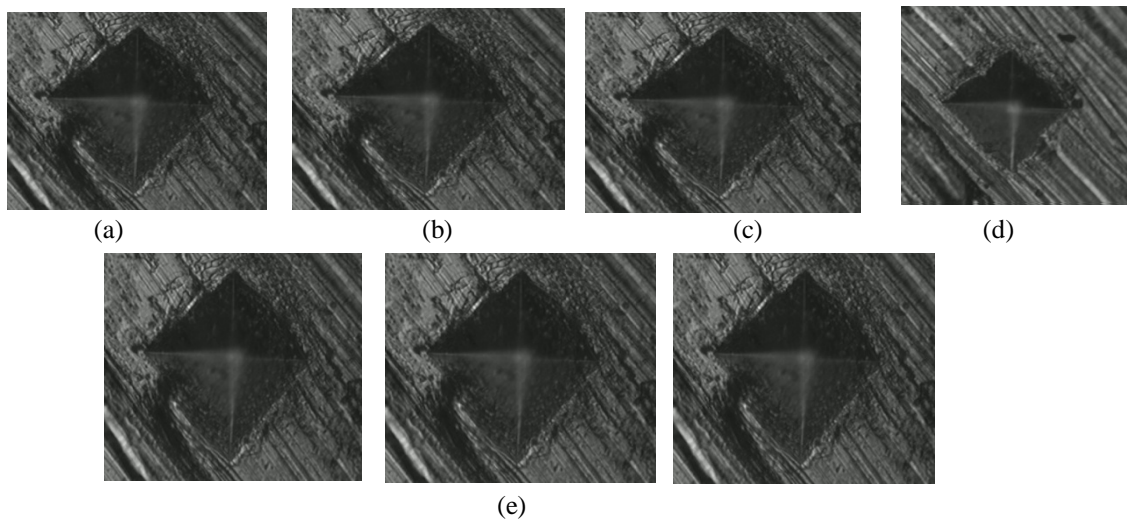


Fig.3. Variation of microhardness of the composite alloy Al-Cd-Pb-Bi over the entire range of experimental growth velocity elocity.

The micromorphological images of the indented specimen of the modal product with different loads, and also with a constant load 50×10^{-2} N at variable induction time are present in figs.4 (a-e). Succinctly, the following inferences are drawn from the combination of figs. 3 and 4 which strongly confirms the plastic deformation of the modal product. The authenticity of the develop micromorphological structure to be the final (modal) product is evidentially verified by determination of its micromechanical parameter relatively upholding the optimum value which obviously be the theoretical strength an experimental extraction that can be visualized in Fig. 3.



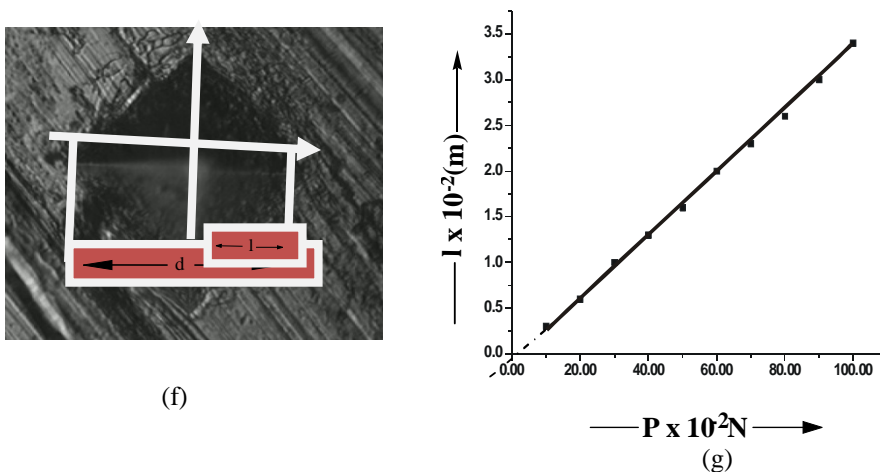


Fig. 4: Photomicrographs showing indentation impressions on modal composite alloy Al-Cd-Pb-Bi under variable

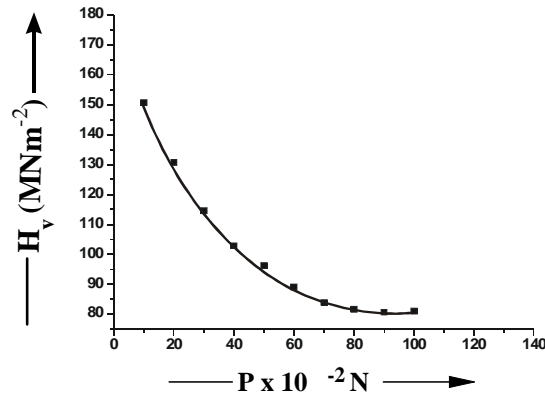
conditions (625 x) (a) size of the indentation with a load of $10 \times 10^{-2} \text{ N}$; (b) size of the indentation with a load of $20 \times 10^{-2} \text{ N}$; (c) size of the indentation with a load of $50 \times 10^{-2} \text{ N}$; (d) size of the indentation with a load of $100 \times 10^{-2} \text{ N}$; (e) invariable size of indentation for a constant applied load of $50 \times 10^{-2} \text{ N}$ at 50, 100 and 150s; (f) measurement of crack length and (g) plot showing variation crack length with applied load.

IV. THEORETICAL EXTRACTION

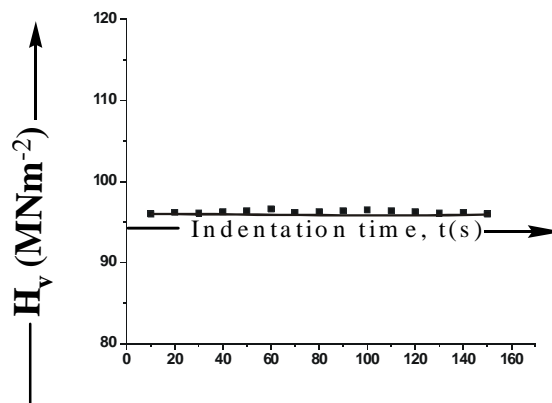
For plastic deformation the Kick's law speaks that micromechanical parameters, H_v remain constant irrespective of the magnitude of a applied load, P Numerically, $P = k_1 d^n$ -----(2) where Meyer's index $n = 2$, accounts for constant H_v , and k_1 is a constant. The literature also indicates the decrease and increase of H_v with rising applied load for materials culminating $n < 2$ and $n > 2$ respectively. Since the hardness whether micro or macro level is the resistance ability of a material to localized permanent deformation, the relationship between the Newtonian resultant pressure W in Newton of the material itself and area of indentation, A in m^2 is the W/A ratio. The Hays and Kendall Hypothesis for plastic deformation, states that the actual load applied to the specimen is $P-W$ in lieu of P . This resultant process of a material represents the minimum applied load to cause indentation as the applied load less than W by definition, will not, result in plastic deformation. This Hypothesis thereupon taking the specimen resistance pressure W into account, modifies Eq. (2) of Kick's law into the following valid form: $(P-W) = k_2 d^2$ -----(3) where k_2 and W are constants. Further, the evaluation of W follows the procedure necessarily involving subtraction of Eq. (2) from Eq. (3) which results in: $d^2 = \left(\frac{k_2}{k_1}\right) d^2 + \frac{W}{k_1}$ ----- (4) The relation yields the parameters W from the theoretical and experimental known values of other parameters defined earlier.

V. EXPERIMENTAL EXTRACTION

The experimental facts obtained are consistent with the theoretical aspects available in the literature for the plastic deformation. The nonlinear relationship between experimental observed, H_v and the applied load P (Fig. 5a) implies that Vickers hardness (H_v) decreases with an increasing applied load until about $70 \times 10^{-2} \text{ N}$ and thereafter, a saturation stage of H_v starts occurring which is full at $80 \times 10^{-2} \text{ N}$.



(a)



(b)

Fig.5: Variation of microhardness for the modal composite alloy Al-Cd-Pb-Bi. (a) Nonlinear with variable applied load at constant indentation time, t (10s). (b) Linear with variable indentation time for constant load P ($50 \times 10^{-2} \text{ N}$)

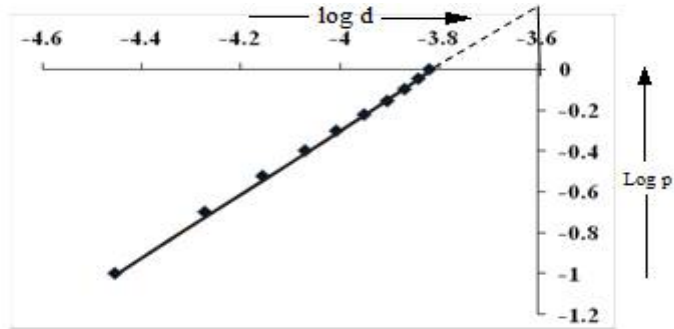
Qualitative explanation of this variation can be suggested that the penetration depth of the indenter with variable applied load is an appropriate consideration to reveal effective rupture of the specimen layers. Comprehensively, the indenter penetrates only surface layers of specimen with small applied load, the effect is more pronounce at these loads. Nevertheless, as the penetration depth increases with the applied varying loads the inner layers' damage of specimen appears to be more effective shattering the ability of hardness to the extent that H_v must become independent of further applied load which actually happened in the experimental range of applied load particular at and beyond $80 \times 10^{-2} \text{ N}$ in the current work. The behavior is consistent with the microhardness increase at loads during early stages of plastic deformation.

International Journal of Innovative Research in Science, Engineering and Technology

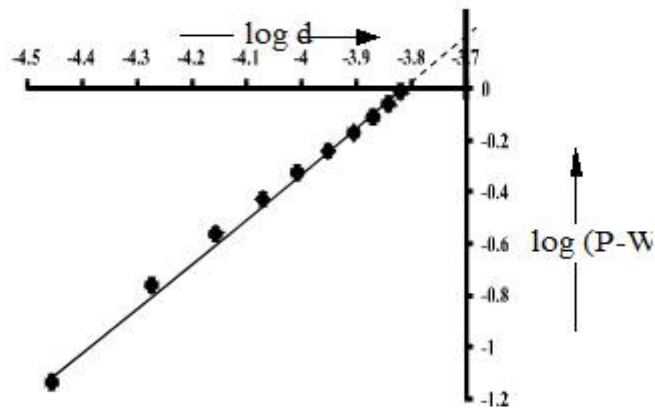
(An ISO 3297: 2007 Certified Organization)

Website: www.ijirset.com

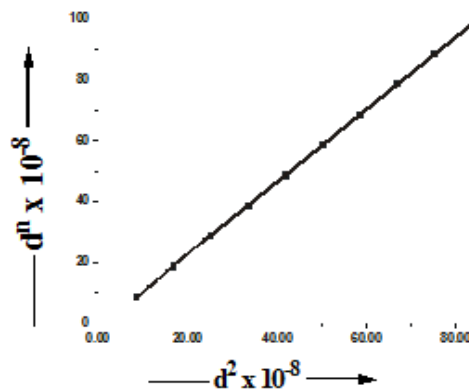
Vol. 6, Issue 2, February 2017



(a)



(b)



(c)

Fig.6: Depiction of relations between the variables (a) log P and log d; (b) log(P-W) and log d and (c) d^n and d^2

International Journal of Innovative Research in Science, Engineering and Technology

(An ISO 3297: 2007 Certified Organization)

Website: www.ijirset.com

Vol. 6, Issue 2, February 2017

A plot between $\log P$ and $\log d$ (Fig.6a) is linear and according to Eq(2) yields n and k_1 for any set of discrete data, the index n being determined by the slope, while the k_1 by the intercept, defined as the particular load P that exists at $d = 10^{-3}$ m. In present investigation, n and k_1 respectively obtained by Fig. 6a are 1.5623 and 1.5135 MPa. Furthermore, plot of $\log (P-W)$ versus $\log d$ of Eq. (3) suggesting the logarithmic index $n=2$, drawn in Fig. 6b yields the value of the logarithmic index, $n < 2$, ($n=1.5623$), thus confirming the validity of the Newtonian resistant pressure theory for the composite specimen, as mentioned earlier, W allows the limiting case to prevail whereat hardness becomes independent of load. Analogically, a plot for d^n ($n=1.5623$) versus d^2 (Fig. 6c) yields the slope k_2/k_1 (0.3086) and W/k_1 ($18.323 \times 10^{-8} \text{ m}^2$) which k_2 and W are separately calculated from the known value of k_1 determined by the plot Fig. 6a, to their respective values 4.903 MPa and 2.7733×10^{-2} N furnishing a compilation of key data on microhardness. Toughness virtually measures the ability of a material absorbing energy up to fracture. Moreover, fracture is a property indicative of material's resistance to fracture when a crack is present. The crack developed on the composite specimen determines the fracture toughness K_c , which specifies the extent to which fracture stress is applied on a uniform loading by the relation: $K_c = \frac{P}{\beta l^{3/2}}$ (5) where l is the radius of a semicircular radial crack or the crack length measured from the centre of the indentation mark to the crack tip. β is a numerical constant that depends on indenter geometry. For a Vickers indenter $\beta = 7$. However, Eq. (5) yields satisfactory values of the fracture toughness only if $l \geq 3$ or $l/a < 3$, respectively for median or radial crack system (Fig. 4f) where 'a' exactly equals half diagonal length, i.e., $a = d/2$. Table 1 records the values of crack length, l and fracture toughness, K_c for the composite specimen at different applied loads. Figure 4(g) is a plot between applied load, P and crack length, l indicating the linear dependence of the crack length on the increasing applied load. Brittleness is an important property, usually termed as the brittleness index B_i , which can be determined from K_c values obeying the relationship: $B_i = \frac{H_v}{K_c}$ (6) the values of B_i obtained from Eq. (6) for the composite specimen at variable microhardness-fracture toughness ratio, are presented in Table 1. The yield strength of the composite computed from the hardness data at variable applied load using the valid equation [9] for $n < 2$: $\sigma_y = \frac{1}{3} H_v$ (7) the values estimated for the composite in the experimental load ranging from 10×10^{-2} to 100×10^{-2} N for an indentation interval of 10 s are also incorporated in Table 1. All the aforesaid parameters are well computable, and their computation collectively, accomplishes inferential analyses that authenticable the plastic deformation of the modal composite Al-Cd-Pb-Bi in the present investigation. Table 1:

S.No	Applied Load P	Crack Length ($l \times 10^{-2}$)	Fracture toughness K_c ($\text{Nm}^{-3/2}$)	Vickers Hardness H_v (MNm^{-2})	Brittleness B_i ($10^6 \text{ m}^{-1/2}$)	Yield strength σ_y (MNm^{-2})
1	10	0.5	40.40	150.63	3.72	50.21
2	20	1.0	28.57	130.72	4.57	43.57
3	30	1.5	23.32	114.62	4.91	38.20
4	40	2.0	20.20	102.93	5.09	34.31
	50	2.5	18.07	96.27	5.32	32.09
6	60	3.0	16.49	89.20	5.40	29.73
7	70	3.5	15.27	83.94	5.49	27.98
8	80	4.0	14.28	81.66	5.71	27.22
9	90	4.5	13.46	80.73	5.99	26.91
10	100	5.0	12.77	81.11	6.34	27.03

These observations are strongly supported by Fig.5b indicating the microhardness of the composite to be independent of variation in the indentation time for a constant load of 50×10^{-2} N at room temperature and revealing the occurrence of plastic deformation which remains unaffected with variable indentation time. Fig.7 shows X-ray patterns of the composite Al-Cd-Pb-Bi. This implies that the X-ray diffraction pattern analysis implicitly, inculcates the existence of the composite as a mechanical mixture of constituent metals simulating weak interactions because of their atomic electronegative character, since no unique diffraction line is exhibited by the composite. The physical significance of

the observations extracted from the X-ray analysis, is that the composite is not a solidus solution but a terminal solidus solution.

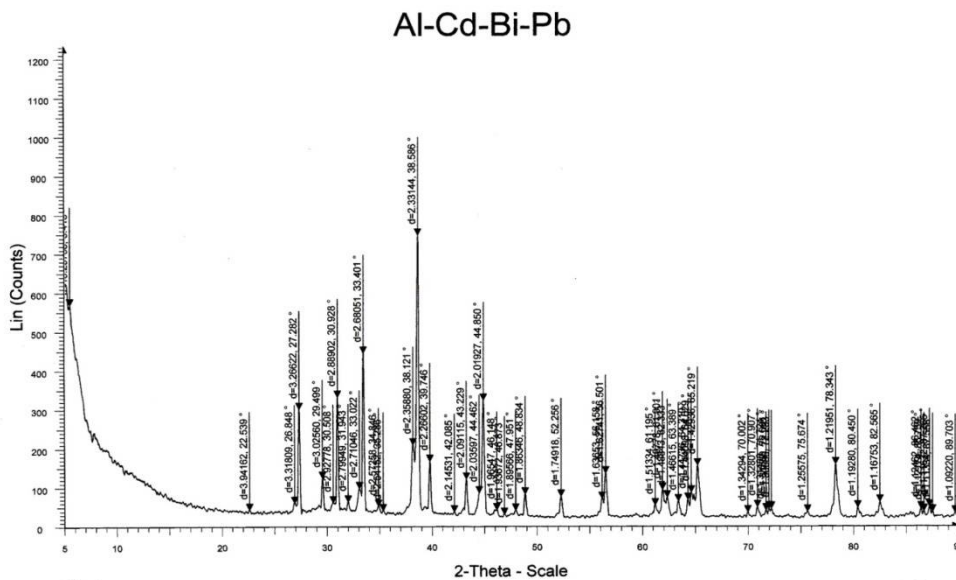


Fig.7: XRD patterns of composite alloy Al-Cd-Pb-Bi.

The concept of occurrence of plastic deformation during modal product testing is further strengthened by theoretical and experimental evidence discussed in the succeeding analyses.

VI. CONCLUSION

Microstructural parameters in the slow and fast growth tend their obedience to the Weibull distribution. However, they start showing deviation in the moderate growth region by alignment which is full at moderate growth velocity ($\sim 2.90 \times 10^{-7} \text{ m}^3 \text{ s}^{-1}$) because of their obedience to the Gauss distribution. The micromechanical parameter (microhardness) of composite in the slow growth is similar, experimental evidence, to that in the fast growth region, but its uniqueness in the moderate region, particularly at the moderate anisotropic growth is a significant aspect of the current work. The microhardness of the composite is found independent of the indentation time but does follow the non-linear dependence with variable applied load. The initiation of the crack on the composite specimen with the required minimum load affirms the applicability of the Newtonian theory of its resistance pressure. The generation of the radial cracks by an indenter loaded with pressure ranging from 10×10^{-2} - 100×10^{-2} N facilitates the procedure to estimate the values of fracture toughness, brittleness index and yield strength of the composite specimen. The inferential significance of the mechanical parameters extracts the concept that the properties of the composite are superior and possibly unique to the properties of the pure constituent metals particularly, when its modal product is achieved by moderate anisotropic growth. Moreover, the physical understanding of the X-ray studies defines the composite to be a terminal solidus solution of the constituent metals stimulating weak interactions at their atomic levels. Thermal analysis reveals thermal stability and liquidus temperatures of the composite.

International Journal of Innovative Research in Science, Engineering and Technology

(An ISO 3297: 2007 Certified Organization)

Website: www.ijirset.com

Vol. 6, Issue 2, February 2017

ACKNOWLEDGEMENT

The author gladly express thanks and acknowledge the instinct cooperative spirit of Mrs. Renu Saini for Computer Assistant and author very thankful to university of Jammu, ISCAS & IIT Roorkee for support of materials & instruments in Laboratory of Research.

REFERENCES

- [1] Arun K Sharma, Parshotam Lal, B K Gandotra, R Kant and B L Sharma, "Anisotropic Mechanical Parameters Microscopic, Thermal and XRD Studies of Ternary Eutectic Composite Phases Sn-Pb-Cd", Arch. Appl. Sci. Res., 4, pp. 111-127, 2012.
- [2] B L Sharma and Parshotam Lal, "Growth Reinforcing Composite Materials from Liquidus Phases: Mechanical and Microstructural Parameters Relationship Essentially Evincing the Predominance of an Akin Mass Composite over the Domain of Composition", Metal, Ceramic and Polymeric Composite for Various uses, John Cuppoletic (Ed.) ISBN, In Tech, 8, pp. 1978-953-307-353, 2012.
- [3] B L Sharma, Parshotam Lal, Monika Sharma and Arun Kumar Sharma, "Thermoanalysis of Binary Condensed Eutectic Phases Evincing Molecular Interaction", J. Therm Anal. Calorim, 8 pp. DOI 10-1007/S/0973-011-1673-8, 2011.
- [4] B L Sharma, R Jamwal and R Kant, Cryst. Res. Technol, 39, pp. 454, 2004.
- [5] B L Sharma, S Tandon and S Gupta, Cryst. Res. Technol., 44, pp. 258-268, 2009.
- [6] B L Sharma, S Gupta, S Tandon and R Kant Mater Chem. Phys., 111, pp. 423-430, 2008.
- [7] D Hull and TW Clyne, "An Introduction to Composite Materials", 2nd edition, 1996.
- [8] D Hull and TW Clyne, "An Introduction to Composite Materials", IIIrd edition, Cambridge University Press, 2008.
- [9] D Hul, "An introduction to composite Materials", Cambridge University Press, Cambridge, 1985.
- [10] DR Lide, "CRC Handbook of Chemistry and Physics, A Ready-Reference Book of Chemical and Physical Data", 90th ed., CRC Press, London, 2009.
- [11] J D Hunt and K A Jackson, Trans., AIME, 236, pp. 843, 1966.
- [12] Parshotam Lal and B L Sharma, "Thermostability, Alloying ability, Growth Habits and Micromechanical Parameters of Aluminium Rich Al-Cd-Sn Composite Alloys", Arch. Appl. Sci. Res., 5, 2012.
- [13] Parshotam Lal, "Characterization of solidus structures of composite materials", Int.J.Adv.Res., 5 (1), pp. 57-65, 2017.
- [14] Parshotam Lal, "Characterization of Binary Composites by X-ray, Thermal and Microscopic studies", Arch. Appl. Sci. Res., 1, 2014.
- [15] Parshotam Lal, Shallu Abrol and BL Sharma, "Essence of Mechanical Properties from Variable Growth Habits of Binary, Ternary and Quaternary Aluminium Rich Alloys", Arch. Appl. Sci. Res., 5, 2012.
- [16] R Caram, M Banan and WR Wilcox, J. Cryst. Growth, 114, pp. 249, 1991.
- [17] R Caram, S Chandrasekha and WR Wilcox, J. Cryst. Growth, 106, pp. 294, 1990.
- [18] R Caram and WR Wilcox, J. Mater. Process, Manuf. Sci, 1, pp. 5, 1992.
- [19] W Albers, "H Muller (Ed.), Preparative Methods of Solid State Chemistry", Academic Press, New York, 1972.
- [20] W D Callister, "Jr., Materials Science and Engineering: An introduction, John Wiley & Sons Inc", 2004.